ARMY RESEARCH LABORATORY

High Shear Strain-Rate Behavior of W-Ni-Fe Tungsten Heavy Alloy Composites as a Function of Matrix Volume Fraction

by Tusit Weerasooriya
and Paul Moy

ARL-TR-1694 May 1998

Army Research Laboratory
Aberdeen Proving Ground, MD 21005-5066

ARL-TR-1694 **May 1998**

High Shear Strain-Rate Behavior of W-Ni-Fe Tungsten Heavy Alloy Composites as a Function of Matrix Volume Fraction

Tusit Weerasooriya, Paul Moy
Weapons and Materials Research Directorate, ARL

Abstract

The effect of matrix volume fraction on the high shear strain-rate deformation and failure behavior of W-Ni-Fe heavy alloys is studied using the torsional Hopkinson bar apparatus. High strain-rate tests (at 700/s) were conducted using torsion specimens made from W-Ni-Fe alloys with three different matrix volume fractions. Different matrix volume fractions were obtained by changing the W content in the W-Ni-Fe alloy while keeping W grain size approximately constant. Experimental observations indicate that as the matrix volume fraction is decreased, the strain to failure decreases, at high rates of loading. There were no significant changes seen in the deformation behavior of the three materials at high shear strain-rate loading used in this study.

Table of Contents

INTENTIONALLY LEFT BLANK

List of Figures

INTENTIONALLY LEFT BLANK

List of Tables

INTENTIONALLY LEFT BLANK

1. Introduction

In a composite such as the tungsten heavy alloy (WHA) examined here, the mechanical properties are heavily dependent on the interfacial strength. WHAs are manufactured by the sintering of W and matrix alloy powders (usually Ni and Fe). This produces a metal matrix composite of pure W particles embedded in a W-Ni-Fe matrix. In a W-Ni-Fe composite, the W-W grain interfaces are far weaker than the W-matrix interfaces [1,2]. During shear (torsional) loading, failure cracks are initiated at this interface by the maximum tensile component of the applied shear load in the plane 45° to the shear loading [3]. Therefore, the mechanical properties of WHAs are dependent on the W-W grain contiguity (defined as the fraction of the W-W interfacial area to the total interfacial area). The initiated cracks at the W-W grain interfaces typically propagate in the direction of the applied shear load, along the matrix, avoiding the hard W grains. Therefore, at high rates of loading, the final failure is dependent not only on W-W grain contiguity, but also on the matrix mean free path of the composite. To fully understand the effect of microstructure on the failure behavior of WHA composites, it is necessary to study the failure as a function of W-W grain contiguity as well as the matrix mean free path, which is a measure of the width of the matrix material separating W-W grains.

Churn et al. [4] studied the effect of the microstructural parameter, the W-W grain contiguity, on the quasi-static tensile and Charpy impact properties. They showed that the ultimate tensile strength and elongation are not dependent on the W-W grain contiguity at the lower rates of loading. However, the W-W grain contiguity parameter has been shown to correlate the change in impact energy obtained from unnotched Charpy tests. These observations were attributed to the lack of change in fracture morphology in quasi-static rate tensile tests and an increase in ductile dimple-type fracture in the Charpy impact tests with decreasing contiguity. Recently, under high shear strain-rate (torsion) loading conditions, failure behavior of a WHA has been studied by Weerasooriya et al. [5] by only changing W-W grain contiguity while keeping the matrix volume fraction (thus, the matrix mean free path width) constant. In this controlled experimental study, it has been observed that the failure shear strain decreased with an increase in W-W grain contiguity. This change in failure strain could be correlated to the change observed in the fracture surface morphology: decreasing ductile dimples and increasing W-W grain boundary facets as the W-W contiguity increased. However, as mentioned previously, the Churn et al. study did not show any change in quasi-static tensile elongation and fracture morphology with change in contiguity.

German and coworkers studied the effect of W content on the tensile properties at quasi-static rates of loading [6,7]. In this case, tensile properties were influenced by both W-W grain contiguity and matrix volume fraction, which influence the initiation and growth of the failure crack, respectively. Since both these parameters vary with the amount of W in the alloy, the reported influence of contiguity on the tensile properties reflects the influence of both the contiguity and matrix volume. With the increase in W content, tensile elongation decreased. The observed correlation was attributed to the formation of cracks in the W-W grain interfaces. This result contradicts the observations by Churn et al., where only the contiguity was varied. At quasi-static rates of loading, tensile failure strains remain unchanged as a function of contiguity when the matrix volume fraction and W grain size are kept constant. However, failure strain changes when both the matrix volume fractions are changed, resulting in variations in both the contiguity and the matrix mean free path. At high rate shear loading and Charpy impact loading, variations in contiguity alone change the strain to failure.

In the application of WHAs as kinetic energy (KE) penetrator materials, they are subjected to high rates of loading. Previous work shows that the deformation and failure characteristics of these alloys are dependent upon the rate of loading [3]. At high shear rates of loading, WHAs can fail by shear localization. Therefore, to understand the effect of contiguity and matrix volume fraction on the WHAs, which are to be used as KE materials, it is necessary to determine their influence at high rates of loading.

The objective of this research is to investigate the effect of matrix volume fraction on the deformation and failure behavior of W-Ni-Fe alloys at high shear rate loading. Matrix volume fraction was varied by changing the W content in the alloy while keeping the W grain size approximately constant and the Ni:Fe ratio at 7:3. WHAs of three different matrix volume fractions with W weight contents of 90, 93, and 96% were used in this study. With a change in W content, both the matrix volume fraction and the contiguity change. Specimens were tested to failure at a high shear loading rate using a torsion Hopkinson bar apparatus. Adhering to careful tolerances, the defect factor of the specimens was restricted to a small range. Defect factor of a torsion specimen, defined by Andrews et al. [8], is a measure of geometric defect or variation in the thickness along the gauge length. Restricting the defect factor of the specimens from the three materials to a small range, the observed differences of the mean values of the deformation and failure behavior of the materials will only depend on the microstructural differences in the alloys. The observed differences in the deformation and failure properties in an alloy are due mainly to the variations in the defect factor of the specimens of that material. Therefore, to extract the effect of microstructure, the key is to machine the specimens with high tolerances so that the variation of the failure properties within a material stays small. With the combination of the experimental data from this program and the data from our previous work, where we varied only the contiguity and kept the matrix volume fraction the same, one should be able to separate the influence of contiguity (a measure of the initiation of failure) and matrix mean free path width (a measure of the propagation of failure) on the high rate failure behavior. A future publication will address this issue after the necessary additional experiments are conducted.

2. Experiments

2.1 Material.

The 17% swaged 90, 93, and 96% W alloys that were used for the experiments in this report were obtained from Teledyne Advanced Materials. The nominal chemical compositions and representative mechanical properties of these alloys are listed in Table 1.

Table 1. Chemical Composition and Mechanical Properties From Manufacturer

Alloy	Chemical Composition			Physical and Mechanical Properties			
	W (%)	Ni (%)	Fe (%)	Density (g/cm^3)	Hardness (R_c)	UTS (MPa)	Elongation (%)
90W-7Ni-3Fe	90.06	6.93	3.02	17.12	37.10	1,091.0	17.9
93W-4.9Ni-2.1Fe	93.04	4.88	2.08	17.70	39.50	1,118.0	17.0
96W-2.8Ni-1.2Fe	96.10	2.79	1.11	18.40	39.30	1,151.5	10.0

Teledyne processed this alloy using the following procedure. An elemental mixture of W, Ni, and Fe powders was cold isostatically pressed at 207 MPa (30,000 psi) in a drybag press. The pressed material was then sintered in a flowing hydrogen atmosphere in a molybdenum wound furnace at 1,520° C. The purpose of the hydrogen atmosphere was to reduce powder surface oxides. The as-sintered material was vacuum-annealed at 1,000° C for 10 hr to remove the absorbed hydrogen. The annealed material was then heated in an inert gas atmosphere to 1,100° C, soaked for 1 hr, then water-quenched to give better dynamic impact properties. The bars were then machined and swaged to a 17% reduction in area.

Figure 1 shows the microstructure of these alloys taken in the longitudinal direction. The microstructure in the transverse direction is similar to that in the longitudinal direction. Swaging up to 17% does not seem to affect the morphology of the microstructure. The microstructure consists of two phases: the spherical grains of nearly pure W with a bcc crystal structure, and a W-Ni-Fe matrix of fcc crystal structure with an approximate composition of 50Ni-25Fe-25W. The relatively brittle W grains are approximately 25–28 mm in diameter. Most of the W grains are surrounded by a thin layer of matrix material, which gives the ductility to the composite. However, some W grains are in contact with adjacent W grains; these areas of contact increase with the W content of the alloy. More detailed quantitative analysis of the microstructures of these three alloys is given in a later section in this report.

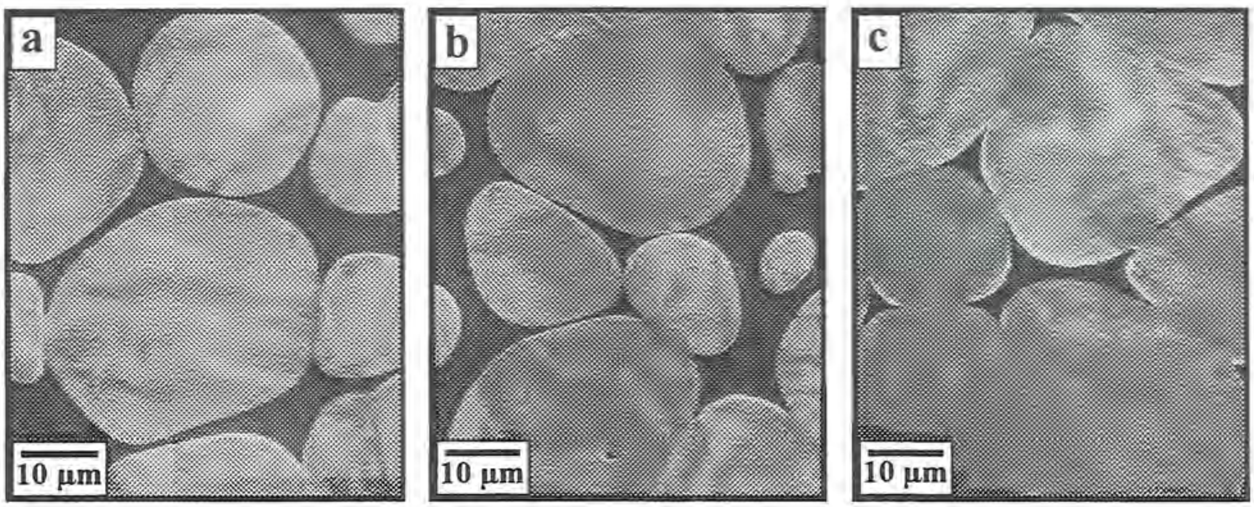

Figure 1. Microstructure of the WHAs Swaged to 17% Reduction in Area. (a) 90, (b) 93, and (c) 96% W, W-Ni-Fe Heavy Alloys.

2.2 Specimen Geometry.

The geometry of the torsional test specimen is shown in Figure 2. The gauge section of the test specimen is a thin wall tube (0.38-mm wall thickness) of 2.540-mm gauge length and outside and inside diameters of 10.16 and 9.40 mm, respectively. The wall thickness corresponds to an average of 14 W grains. Hexagonal flanges with 60° shoulders are machined at both ends of the thin tubular gauge section and are used to attach the specimen to the elastic input and output bars of the test system. After initially machining the inside and outside diameters of the gauge section to 0.25 mm undersize and oversize, respectively, the specimens were machined to the final dimensions with the specified tolerances by honing the inside and grinding and polishing the outside. Grinding is also employed to obtain a radius of approximately 0.38 mm between the shoulder and the gauge area. With the careful machining of the specimens to the specified tolerances, the defect factor of the gauge area of all the specimens is forced to lie within a small range.

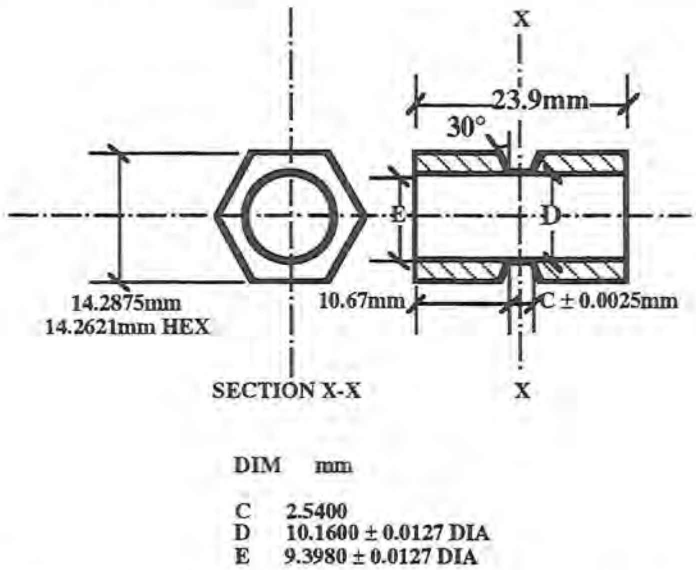

Figure 2. Dimensions and Tolerances of the Torsion Hopkinson Bar Specimen.

Using this short gauge length specimen with 60° shoulders, an almost homogeneous state of strain is achieved after a few reflections of the applied shear stress pulse. In a specimen with the same gauge area dimensions, but with end flanges with sharper (90°) shoulders, the plastic zone starts at the flange-gauge section interface. Although the plastic zone starts at this interface, it spreads gradually through the specimen and engulfs the whole gauge section [9].

2.3 Quantitative Microstructural Analysis of the WHAs.

Quantitative microstructural values, matrix volume fraction, W-W grain contiguity, matrix mean free path width, and W grain size for the three alloys are obtained by image analysis of the optical micrographs. Digitally scanned images of the micrographs were analyzed using Image 1.47 software from the National Institutes of Health on a Macintosh computer. For each WHA, micrographs from five different locations are used for the image analysis. Table 2 gives the results of the quantitative microstructural analysis with standard deviations. The matrix volume fractions, defined as the ratio of the total area of the matrix and the total area of the micrograph, of the 90, 93, and 96% W content WHAs are 0.23, 0.14, and 0.09, respectively. One would expect, as the W content increases, matrix volume fraction decreases. Matrix mean free path width is defined as the total matrix area divided by two times the difference between the total length of W grain perimeters and the total length of W-W grain contacts. This width defines the average thickness of the matrix material in a WHA micrograph; the failure crack would propagate through this matrix material. For the three alloys of 90, 93, and 96% W, the average matrix mean free path widths are 0.81, 0.57, and 0.45 μm, respectively, decreasing with increasing W content. W-W grain contiguity in Table 2 is defined as the ratio of the total length of W-W grains in contact with each other to the total circumferential lengths of the W grains in the micrographs. The W-W grain contact is the weakest interface and therefore is the most probable failure initiation location. Using this definition of contiguity, 90, 93, and 96% W alloys have mean contiguities of 0.15, 0.29, and 0.41 respectively. W grain sizes are calculated as the square root of four times the total W grain area divided by the value of π times the total number of W grains. The grain sizes for the three materials are very similar, with the average grain sizes ranging from 24.48 to 28.14 mm.

Table 2. Quantitative Microstructural Data for the Three Alloys

Microstructural Parameters	90W-7Ni-3Fe		93W-4.9Ni-2.1Fe		96W-2.8Ni-1.2Fe	
	Mean	Std. Deviation	Mean	Std. Deviation	Mean	Std. Deviation
Matrix Volume Fraction	0.23	0.03	0.15	0.02	0.09	0.03
W-W Grain Contiguity	0.15	0.05	0.29	0.04	0.41	0.07
Matrix Mean Free Path Width (mm)	0.81	0.11	0.57	0.04	0.45	0.12
W Grain Size (mm)	25.23	4.16	28.14	2.07	24.48	2.43

2.4 Test Apparatus.

The high rate tests were conducted using a torsional split-Hopkinson bar. The original apparatus was developed by Kolsky to conduct compression tests at high loading rates. This apparatus was later modified to conduct torsion tests by Baker and Yew [10] and Duffy et al. [11]. The torsional Hopkinson bar used to conduct these experiments was based on the apparatus developed by Duffy et al. [12]. A schematic of the torsional Hopkinson bar is given in Figure 3. It consists of two 7075-T6 aluminum bars of diameter 25.4 mm and length 2,438 mm. The hexagonal flanged thin wall specimen is attached between the two bars. A torque is stored between the non-specimen end of the input bar and the clamp. The high strain-rate of loading is applied to the specimen by the sudden release of the stored torque by breaking the clamp. The position of the clamp on the input bar relative to the loading pulley determines the duration of the stress pulse. This incident torsional stress pulse travels toward the specimen after its release; at the specimen, part of the pulse transmits through the specimen to the output bar, and the remainder reflects back to the input bar. From the incident, reflected, and transmitted pulses measured using strain gauges mounted on the input and output bars, the stress, strain, and strain rate can be inferred as a function of time. The details of the data acquisition and reduction procedure are similar to those given by Weerasooriya [13]. When a shear band initiates, the strain and strain rate that are determined by this method represent average values in the gauge section of the specimen.

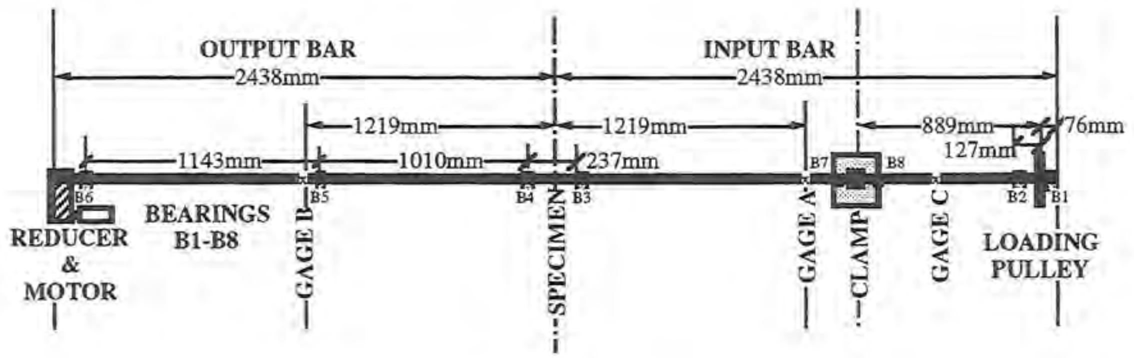

Figure 3. Schematic of the Torsional Split-Hopkinson Bar.

2.5 Test Method.

High rate torsion tests were conducted on specimens from the 90, 93, and 96% W heavy alloys using the torsional Hopkinson bar apparatus. All the tests were conducted to failure at an average strain-rate of approximately 700/s. Data from the tests were reduced to obtain the stress-strain behavior of the material and the failure stress and strain.

3. Results and Discussion

The reflected and transmitted stress pulses measured in each of the tests are reduced to obtain the stress-strain plots shown in Figures 4, 5, and 6. The method used to reduce data is described elsewhere [13]. The initial transients in the stress-strain plots are artifacts of the high rate testing method.

Reduced stress-strain data from the specimens from 90% W WHA are shown in the Figure 4. The stress-strain data show that prior to an average total shear strain of 0.144, the material work-hardened. After that point (instability strain), material seems to soften with increasing strain.

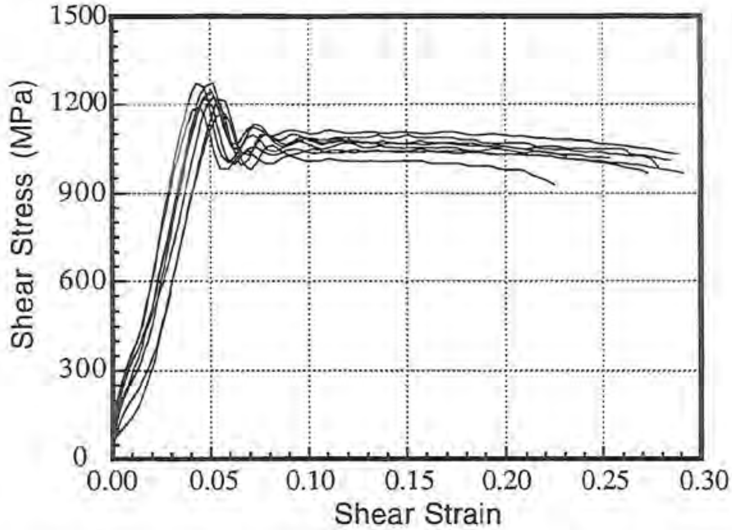

Figure 4. Stress-Strain Curves up to Failure for 90% W WHA at 700/s.

Figure 5 shows the reduced stress-strain data at 700/s strain-rate from 93% W WHA specimens. As in the 90% W material, the material began work softening with increasing strain, beyond an average strain of 0.11.

Figure 6 shows the reduced stress-strain data at 700/s strain-rate from 96% W WHA specimens. This material starts to work-soften at shear strains above a mean strain of 0.105.

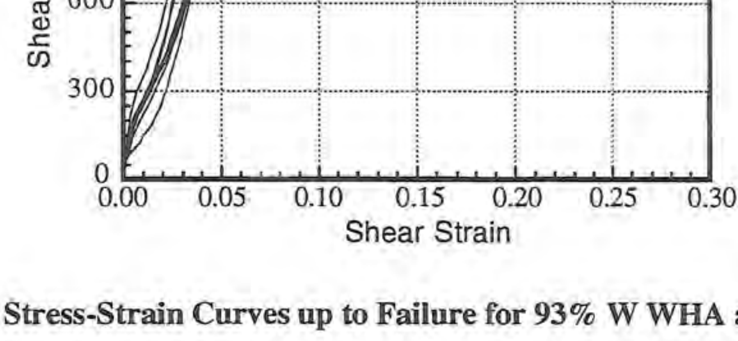

Figure 5. Stress-Strain Curves up to Failure for 93% W WHA at 700/s.

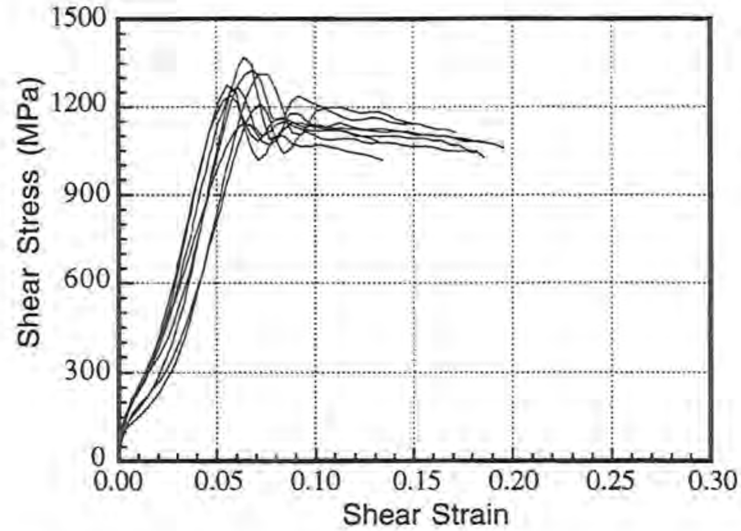

Figure 6. Stress-Strain Curves up to Failure for 96% W WHA at 700/s.

Table 3 shows a comparison of failure strains, failure stresses, yield stresses, and strains at the maximum stress (instability strain) for the three alloys. Because of the initial ringing in the stress-strain data, the reported yield stresses are determined from extrapolating the stress-strain curves through the initial overshoot back to the linear portion and then taking a 0.2% offset from the linear portion. The material with highest W content, the 96% W alloy, has a mean extrapolated yield strength of 1128.7 MPa; and the yield strengths of 93 and 90% W alloys are 1023.8 and 1056.5 MPa, respectively. The dynamic yield stress does not appear to be dependent on the W content, and hence on the matrix volume, with any statistical significance. Mean failure strengths of the material with 96, 93 and 90% W contents are 1069.0, 983.9, and 1003.9 MPa, respectively. There is no statistically significant trend in failure strength as a function of matrix volume as well. Mean failure strains for the 96, 93, and 90% alloys are 0.16, 0.21, and 0.26, respectively; their respective standard deviations are 0.02, 0.03, and 0.02. Variations in failure strain within one material is attributed to the variation in the defect factor of the specimen gauge section (function of the tolerances used in machining of the specimen). But the variation in the mean values of the failure strain between different materials is due to the differences in the material microstructure. Failure strains of all the specimens from the three alloys are shown in Figure 7. Lower matrix volume fraction materials failed earlier than the higher matrix volume fraction materials with a very high probability (a statistically insignificant probability of 0.0003 for 90 and 93% W material to fail at the same level of strain, and a statistically insignificant probability of 0.0005 for 93 and 96% W materials to fail at the same level of strain). Therefore, it can be concluded with certainty that as the matrix volume fraction of W-Ni-Fe heavy alloy increases, the failure strain under high shear strain-rate loading also increases. As seen in Figure 8, the relationship between mean failure strain and the matrix volume fraction is linear (correlation coefficient, $R = 0.99853$). Instability strains for the three materials are approximately the same and therefore are not dependent on matrix volume fraction.

Table 3. Yield Stress, Failure Strain, and Failure Stress Data From the High Strain-Rate Torsion Experiments

Alloy (matrix volume fraction)	Yield Stress (MPa)		Failure Strain		Failure Stress (MPa)		Strain @ Maximum Stress	
	Mean	Std. Deviation	Mean	Std. Deviation	Mean	Std. Deviation	Mean	Std. Deviation
90W-7Ni-3Fe (0.23)	1056.5	29.5	0.26	0.02	1003.9	36.9	0.14	0.02
93W-4.9Ni-2.1Fe (0.15)	1023.8	46.5	0.21	0.03	983.9	37.3	0.11	0.01
96W-2.8Ni-1.2Fe (0.09)	1128.7	44.8	0.16	0.02	1069.0	43.6	0.11	0.01

From our previous work, it has been found that the W-Ni-Fe heavy alloy torsion specimens fail by the initiation and growth of a shear localization [3]; the localized instability initiated by the opening of the cavities at W-W grain interfaces and then grew along the matrix. The reason for the early shear failure of the lower matrix volume fraction material is the presence of larger W-W grain interfaces and earlier failures at these interfaces. Cracks form easily at these interfaces. Separated W-W grain interfacial cracks act as the stress concentrators for an early localized shear failure. In our earlier high rate torsion work on the unheat-treated material, the fracture surfaces of the failed specimens reveal W-W grain interface failure. When the W grains are separated with a thin layer of matrix material, as in the case of a low contiguity material, the initial cracks have to start at the matrix-W grain interface or at the remaining small W-W grain interface. It takes a larger strain to initiate cracks at this W-matrix interface; the cracks that initiate at the remaining smaller W-W grain contacts will naturally be much smaller in size and therefore have a smaller stress intensity factor than the cracks in a higher contiguity material where the crack lengths formed at W-W grain separation are larger. Thus, the cracks started in a lower contiguity material require a larger strain to propagate.

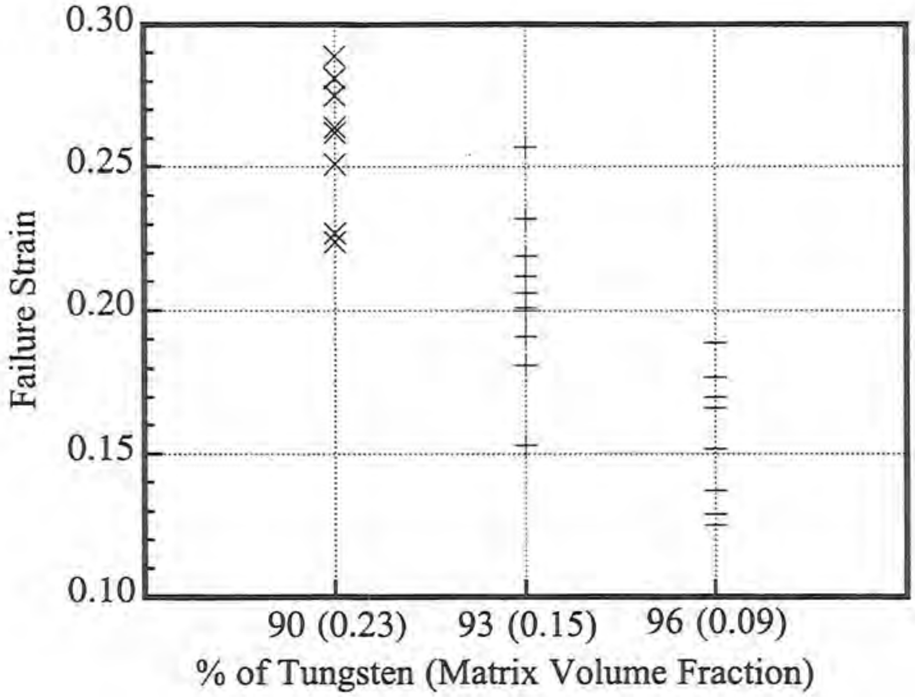

Figure 7. Comparison of Shear Strains to Failure for WHAs With Three Different W Contents (Matrix Volume Fractions).

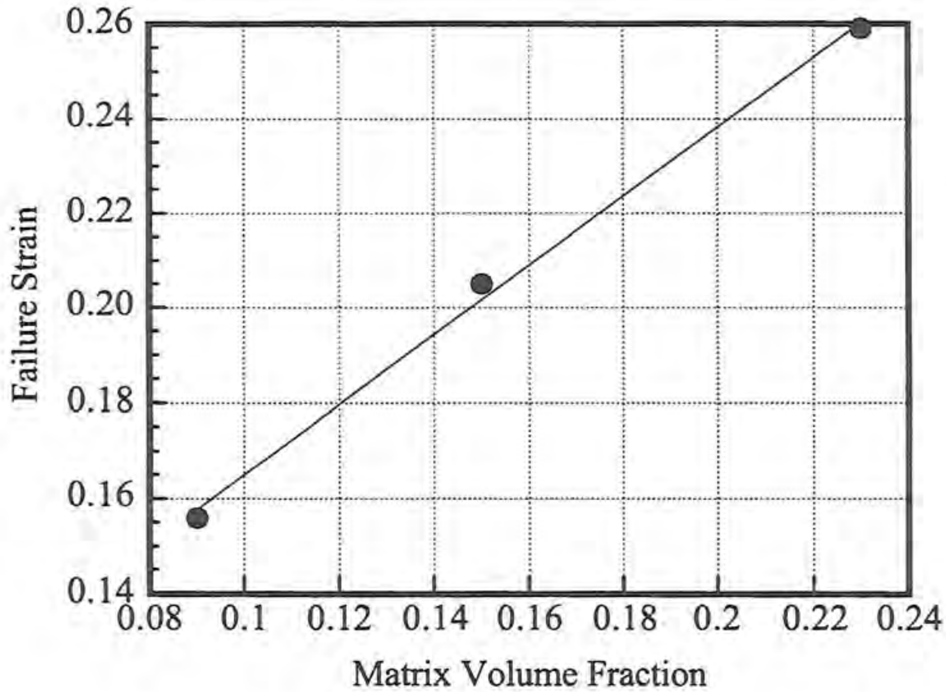

Figure 8. Shear Strains to Failure for WHAs With Three Different W Contents Plotted as a Function of Their Matrix Volume Fractions.

Figure 9 shows typical fracture surface morphologies from specimens from the three materials with differing matrix volume fractions. The fracture surface of the specimens from low matrix volume fraction material consists of brittle cleavage fracture surfaces of W grains, brittle W-W interfacial separation zones, and typical smooth shear localization zones as shown in Figure 9(c). In addition to these types of fracture zones, ductile dimple-type separation zones of matrix material are also present in the specimens from higher matrix volume (Figure 9 [a and b]). This is expected due to the presence of lesser amount of W-W grain interfacial zones in the material with higher matrix volume fractions.

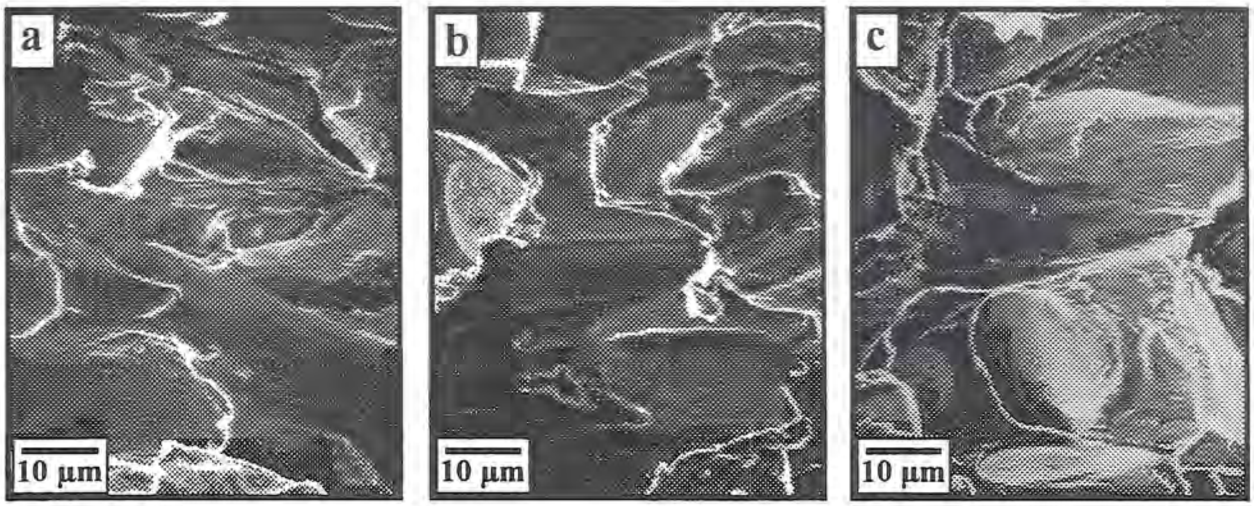

Figure 9. Typical Fracture Surface Morphologies From (a) High, (b) Intermediate, and (c) Low Matrix Volume Fraction WHAs.

4. Summary and Conclusions

The effect of matrix volume fraction on high shear strain-rate deformation and failure behavior of three W-Ni-Fe heavy alloys were studied using a torsional Hopkinson bar apparatus. High strain-rate tests (at 700/s) were conducted to failure on torsion specimens made from materials with three different W contents: 90, 93, and 96%. After the tests, all the fracture surfaces of the specimens were analyzed using a scanning electron microscope.

At the loading rate used in the tests, increasing the matrix volume fraction increases strain to failure linearly. There are no significant differences in the deformation behavior (flow stress) of the three materials. The observed increase in failure strain with increasing matrix volume fraction is attributed to the decrease in zones of brittle failure mode. In the specimens from the material with lowest matrix volume fraction, the fracture surface of the specimens shows cleavage of W grains, brittle failure at the W-W grain interfaces, and smooth zones, indicating shear localization. There were dimple-type ductile matrix fracture zones in the material from higher matrix volume fractions in addition to the cleaved W grains, brittle W-W interface separation zones, and smooth shear localized zones.

INTENTIONALLY LEFT BLANK

5. References

1. Churn, K. S., and D. N. Yoon. "Pore Formation and its Effect on Mechanical Properties in W-Ni-Fe Heavy Alloy." *Powder Metallurgy*, vol. 22, pp. 175–178, 1979.

2. Ekbom, L. "Influence of Microstructure of Liquid-Sintered Tungsten-Base Composites on the Mechanical Properties." *Scandinavian Journal of Metallurgy*, vol. 5, pp. 179–184, 1976.

3. Weerasooriya, T., and P. A. Beaulieu. "Effects of Strain-Rate on the Deformation and Failure Behavior of 93W-5Ni-2Fe Under Shear Loading." *Material Science and Engineering*, vol. A172, pp. 71–78, 1993.

4. Churn, K. S., J. W. Noh, H. S. Song, E. P. Kim, S. Lee, and W. H. Baek. "The Effect of Contiguity on the Mechanical Properties of 93W-5.6Ni-1.4Fe Heavy Alloy." *Proceedings of International Conference on Tungsten and Tungsten Alloys*, Metal Powder Industries Federation, pp. 397–405, edited by A. Bose and R. J. Dowding, McLean, VA, 1992.

5. Weerasooriya, T., P. Moy, and R. J. Dowding. "Effect of W-W Grain Contiguity on the High Shear Strain-Rate Behavior of 93W-5Ni-2Fe Tungsten Heavy Alloy." *Proceedings of the 2nd International Conference on Tungsten and Refractory Metals,* Metal Powder Industries Federation, pp. 401–409, edited by A. Bose and R. J. Dowding, McLean, VA, 1994.

6. Churn, K. S., and R. M. German. "Fracture Behavior of W-Ni-Fe Heavy Alloys." *Metallurgical Transaction A*, vol. 15A, pp. 331–338, 1984.

7. Rabin, R. H., and R. M. German. "Microstructure Effects on Tensile Properties of Tungsten-Nickel-Iron Composites." *Metallurgical Transaction A*, vol. 19A, pp. 1523–1532, 1988.

8. Andrews, E. W., A. F. Bower, and J. Duffy. "Shear Band Formation in a Tungsten Heavy Alloy." *Proceedings Symposium on Shear Bands and Viscoplastic Theories*, The 29th Annual Technical Meeting of the Society for Engineering Science, La Jolla, CA, September 1992.

9. Leung, E. K. C. "An Elastic-Plastic Stress Analysis of the Specimen Used in the Torsional Kolsky Bar." *Journal of Applied Mechanics*, vol. 47, p. 278, 1980.

10. Baker, W. W. "Strain-rate Effects in the Propagation of Torsional Plastic Waves." *Journal of Applied Mechanics*, vol. 33, p. 917, 1966.

11. Duffy, J., J. D. Campbell, and R. H. Hawley. "On the Use of a Torsional Split-Hopkinson Bar to Study Rate Effects in 1100-0 Aluminum." *Journal of Applied Mechanics*, vol. 38, p. 83, 1971.

12. Duffy, J., J. Hartley, and R. H. Hawley. "The Torsional Kolsky (Split-Hopkinson) Bar, High Rate Testing." *Metals Handbook*, American Society for Metals, vol. 8, p. 2168, 1985.

13. Weerasooriya, T. "MTL Torsional Hopkinson Bar." MTL TR 90-27, U.S. Army Materials Technology Laboratory, Watertown, MA, 1990.

INTENTIONALLY LEFT BLANK

NO. OF COPIES	ORGANIZATION
2	DEFENSE TECHNICAL INFORMATION CENTER DTIC DDA 8725 JOHN J KINGMAN RD STE 0944 FT BELVOIR VA 22060-6218
1	HQDA DAMO FDQ DENNIS SCHMIDT 400 ARMY PENTAGON WASHINGTON DC 20310-0460
1	DPTY ASSIST SCY FOR R&T SARD TT F MILTON RM 3EA79 THE PENTAGON WASHINGTON DC 20310-0103
1	OSD OUSD(A&T)/ODDDR&E(R) J LUPO THE PENTAGON WASHINGTON DC 20301-7100
1	CECOM SP & TRRSTRL COMMCTN DIV AMSEL RD ST MC M H SOICHER FT MONMOUTH NJ 07703-5203
1	PRIN DPTY FOR TCHNLGY HQ US ARMY MATCOM AMCDCG T M FISETTE 5001 EISENHOWER AVE ALEXANDRIA VA 22333-0001
1	DPTY CG FOR RDE HQ US ARMY MATCOM AMCRD BG BEAUCHAMP 5001 EISENHOWER AVE ALEXANDRIA VA 22333-0001
1	INST FOR ADVNCD TCHNLGY THE UNIV OF TEXAS AT AUSTIN PO BOX 202797 AUSTIN TX 78720-2797

NO. OF COPIES	ORGANIZATION
1	GPS JOINT PROG OFC DIR COL J CLAY 2435 VELA WAY STE 1613 LOS ANGELES AFB CA 90245-5500
3	DARPA L STOTTS J PENNELLA B KASPAR 3701 N FAIRFAX DR ARLINGTON VA 22203-1714
1	US MILITARY ACADEMY MATH SCI CTR OF EXCELLENCE DEPT OF MATHEMATICAL SCI MDN A MAJ DON ENGEN THAYER HALL WEST POINT NY 10996-1786
1	DIRECTOR US ARMY RESEARCH LAB AMSRL CS AL TP 2800 POWDER MILL RD ADELPHI MD 20783-1145
1	DIRECTOR US ARMY RESEARCH LAB AMSRL CS AL TA 2800 POWDER MILL RD ADELPHI MD 20783-1145
3	DIRECTOR US ARMY RESEARCH LAB AMSRL CI LL 2800 POWDER MILL RD ADELPHI MD 20783-1145
	ABERDEEN PROVING GROUND
4	DIR USARL AMSRL CI LP (305)

NO. OF COPIES	ORGANIZATION
1	COMMANDER US ARMY ARDEC G FLEMING PICATINNY ARSENAL NJ 07806-5000
2	COMMANDER US ARMY ARDEC AMSTA AR FSA E E BAKER D KAPOOR PICATINNY ARSENAL NJ 07806-5000
2	SOUTHWEST RSRCH INSTITUTE C ANDERSON J LANKFORD PO DRAWER 28510 SAN ANTONIO TX 78228-0510
1	DIRECTOR LOS ALAMOS NATIONAL LAB MS B296 G T GRAY PO BOX 1663 LOS ALAMOS NM 87545
1	AIR FORCE WRIGHT LAB TECH LIB J FOSTER ARMAMENT DIVISION 101 EGLIN AVE STE 239 EGLIN AFB FL 32542
1	LOS ALAMOS NATIONAL LAB D RABERN GROUP MEE 13 MSJ576 LOS ALAMOS NM 87545
1	LOS ALAMOS NATIONAL LAB TECH LIB PO BOX 1663 LOS ALAMOS NM 87545
1	JOHNS HOPKINS UNIVERSITY DEPT MECH ENGINEERING K RAMESH CHARLES AND 33 ST BALTIMORE MD 21218
1	PENN STATE UNIVERSITY COLLEGE OF ENGINEERING R GERMAN UNIVERSITY PARK PA 16802-6809

NO. OF COPIES	ORGANIZATION
1	BROWN UNIVERSITY DIV OF ENGINEERING R CLIFTON PROVIDENCE RI 02912
1	UC SAN DIEGO DEPT APPL MECH AND ENG SVCS R011 S NEMAT-NASSER LA JOLLA CA 92093-0411
1	CALTECH G RAVICHANDRAN MS 105-50 1201 E CALIFORNIA BLVD PASADENA CA 91125
1	INST OF ADVANCE TECH UNIV OF TX AUSTIN S J BLESS 4030 2 W BRAKER LN AUSTIN TX 78759
1	COMMANDER US ARMY RSRCH OFFC K IYER PO BOX 12211 RESEARCH TRIANGLE PARK NC 27709-2211
1	VIRGINIA POLYTECHNIC INST COLLEGE OF ENGNR R BATRA BLACKSBURG VA 24061-0219
1	DIR LLNL D LASILA L170 LIVERMORE CA 94550

ABERDEEN PROVING GROUND

NO. OF COPIES	ORGANIZATION
56	DIR USARL AMSRL WM TD S CHOU A M DIETRICH D DANDEKAR A RAJENDRAN T HADUCH S SCHOENFELD K FRANK M RAFTENBERG J WALTERS T WRIGHT P KINGMAN S SEGLETES T WEERASOORIYA (15 CPS)

NO. OF COPIES	ORGANIZATION
	AMSRL WM TC W DEROSSET T BJERKE E KENNEDY R MUDD W WALTERS L MAGNESS R COATES B SORENSON D SCHEFFLER K KIMSEY AMSRL WM TA W GILLICH W BRUCHEY M BURKINS E RAPACKI N RUPERT J RUNYEON W A GOOCH G FILBEY AMSRL WM MA R SHUFORD L GHIORSE S MCKNIGHT AMSRL WM MC R ADLER M STAKER G KRASKO AMSRL WM MD R DOWDING K CHO AMSRL WM MB B BURNS C HOPPEL G GAZONAS

INTENTIONALLY LEFT BLANK.

REPORT DOCUMENTATION PAGE

Form Approved
OMB No. 0704-0188

1. AGENCY USE ONLY *(Leave blank)*

2. REPORT DATE
May 1998

3. REPORT TYPE AND DATES COVERED
Final, Jan 95 - May 98

4. TITLE AND SUBTITLE
High Shear Strain-Rate Behavior of W-Ni-Fe Tungsten Heavy Alloy Composites as a Function of Matrix Volume Fraction

5. FUNDING NUMBERS
PR: 1L162618AH80

6. AUTHOR(S)
Tusit Weerasooriya and Paul Moy

7. PERFORMING ORGANIZATION NAME(S) AND ADDRESS(ES)
U.S. Army Research Laboratory
ATTN: AMSRL-WM-TD
Aberdeen Proving Ground, MD 21005-5066

8. PERFORMING ORGANIZATION REPORT NUMBER
ARL-TR-1694

9. SPONSORING/MONITORING AGENCY NAMES(S) AND ADDRESS(ES)

10.SPONSORING/MONITORING AGENCY REPORT NUMBER

11. SUPPLEMENTARY NOTES

12a. DISTRIBUTION/AVAILABILITY STATEMENT
Approved for public release; distribution is unlimited.

12b. DISTRIBUTION CODE

13. ABSTRACT *(Maximum 200 words)*

The effect of matrix volume fraction on the high shear strain-rate deformation and failure behavior of W-Ni-Fe heavy alloys is studied using the torsional Hopkinson bar apparatus. High strain-rate tests (at 700/s) were conducted using torsion specimens made from W-Ni-Fe alloys with three different matrix volume fractions. Different matrix volume fractions were obtained by changing the W content in the W-Ni-Fe alloy while keeping W grain size approximately constant. Experimental observations indicate that as the matrix volume fraction is decreased, the strain to failure decreases, at high rates of loading. There were no significant changes seen in the deformation behavior of the three materials at high shear strain-rate loading used in this study.

14. SUBJECT TERMS
tungsten heavy alloy; matrix volume fraction; high strain rate; torsion; failure

15. NUMBER OF PAGES
23

16. PRICE CODE

17. SECURITY CLASSIFICATION OF REPORT	18. SECURITY CLASSIFICATION OF THIS PAGE	19. SECURITY CLASSIFICATION OF ABSTRACT	20. LIMITATION OF ABSTRACT
UNCLASSIFIED	UNCLASSIFIED	UNCLASSIFIED	UL

INTENTIONALLY LEFT BLANK.

USER EVALUATION SHEET/CHANGE OF ADDRESS

This Laboratory undertakes a continuing effort to improve the quality of the reports it publishes. Your comments/answers to the items/questions below will aid us in our efforts.

1. ARL Report Number/Author ARL-TR-1694 (Weerasooriya) Date of Report May 1998

2. Date Report Received ______

3. Does this report satisfy a need? (Comment on purpose, related project, or other area of interest for which the report will be used.) ______

4. Specifically, how is the report being used? (Information source, design data, procedure, source of ideas, etc.) ______

5. Has the information in this report led to any quantitative savings as far as man-hours or dollars saved, operating costs avoided, or efficiencies achieved, etc? If so, please elaborate. ______

6. General Comments. What do you think should be changed to improve future reports? (Indicate changes to organization, technical content, format, etc.) ______

CURRENT ADDRESS

Organization

Name E-mail Name

Street or P.O. Box No.

City, State, Zip Code

7. If indicating a Change of Address or Address Correction, please provide the Current or Correct address above and the Old or Incorrect address below.

OLD ADDRESS

Organization

Name

Street or P.O. Box No.

City, State, Zip Code

(Remove this sheet, fold as indicated, tape closed, and mail.)

(DO NOT STAPLE)

DEPARTMENT OF THE ARMY

OFFICIAL BUSINESS

NO POSTAGE
NECESSARY
IF MAILED
IN THE
UNITED STATES

BUSINESS REPLY MAIL
FIRST CLASS PERMIT NO 0001,APG,MD

POSTAGE WILL BE PAID BY ADDRESSEE

DIRECTOR
US ARMY RESEARCH LABORATORY
ATTN AMSRL WM TD
ABERDEEN PROVING GROUND MD 21005-5066